Chemical Science

ROYAL SOCIETY OF CHEMISTRY

EDGE ARTICLE

View Article Online
View Journal | View Issue

Cite this: *Chem. Sci.*, 2023, **14**, 10971

All publication charges for this article have been paid for by the Royal Society of Chemistry

Received 1st August 2023
Accepted 12th September 2023

DOI: 10.1039/d3sc03987k

rsc.li/chemical-science

Rh(III)-catalyzed highly site- and regio-selective alkenyl C–H activation/annulation of 4-amino-2-quinolones with alkynes *via* reversible alkyne insertion†

Naohiro Hirako, Takeshi Yasui * and Yoshihiko Yamamoto *

3,4-Fused 2-quinolone frameworks are important structural motifs found in natural products and biologically active compounds. Intermolecular alkenyl C–H activation/annulation of 4-amino-2-quinolone substrates with alkynes is one of the most efficient methods for accessing such structural motifs. However, this is a formidable challenge because 4-amino-2-quinolones have two cleavable C–H bonds: an alkenyl C–H bond at the C3-position and an aromatic C–H bond at the C5-position. Herein, we report the Rh(III)-catalyzed highly site-selective alkenyl C–H functionalization of 4-amino-2-quinolones to afford 3,4-fused 2-quinolones. This method has a wide substrate scope, including unsymmetrical internal alkynes, with complete regioselectivity. Several control experiments using an isolated key intermediate analog suggested that the annulation reaction proceeds *via* reversible alkyne insertion involving a binuclear Rh complex although alkyne insertion is generally recognized as an irreversible process due to the high activation barrier of the reverse process.

Introduction

Transition-metal-catalyzed site-selective C–H functionalization with the aid of directing groups is one of the most powerful methods of accessing complex molecules from readily available starting materials with high efficiency.[1] The Rh(III)-catalyzed oxidative annulation of aromatic compounds with alkynes *via* C–H activation has been recognized as an efficient method of synthesizing fused carbo- and heterocycles such as naphthalenes, isoquinolones, isoquinolines, indoles, and isocoumarins.[2] However, the site-selective C–H functionalization of aromatic compounds with multiple cleavable C–H bonds, such as the *ortho* and *peri* C–H bonds of the naphthalene ring, remains a challenge. Several research groups have addressed this issue by developing Rh(III)-catalyzed site-selective functionalizations of such aromatic compounds.[3] For example, Jin *et al.* reported the Rh(III)-catalyzed site-selective C–H functionalization of 1-naphthylcarbamates (Scheme 1a).[4] In this reaction, a neutral Rh(III) catalyst enabled *peri* C–H activation *via* selective coordination to the carbamate nitrogen, while a cationic Rh(III) catalyst selectively activated the *ortho* C–H bond *via* coordination to the carbamate oxygen in preference to the nitrogen due to its Lewis acidity. In contrast, the C–H functionalization of aromatic heterocycles is more complicated because these heterocycles usually have a greater electronic bias than aromatic carbocycles such as benzene and naphthalene.[5] For example, Huckins, Bercot, *et al.* reported that the C–H functionalization of pyridine *N*-oxides proceeds selectively at the C2-position, whereas the reaction of the corresponding pyridine analog proceeds with poor site-selectivity (Scheme 1b).[6a] The computational mechanistic study conducted by Huckins, Thiel, Houk, *et al.* elucidated that the electrostatic interaction between the substrates and alkynes is the pivotal factor affecting the selectivity, whereas the selectivity-determining step can be either C–H activation or alkyne insertion depending on alkynes used.[6b] However, mechanistic studies to gain insight into the principles behind such selectivity in the C–H functionalization of aromatic heterocycles have rarely been conducted.

2-Quinolone derivatives fused at the C3- and C4-positions are important motifs found in natural products and biologically active substances.[7] The annulation reaction of 2-quinolones involving C–H activation is one of the most efficient methods of preparing 3,4-fused 2-quinolones such as indoloquinolones.[8] In particular, the intermolecular annulation of 2-quinolones is highly desirable, as substrates are readily available compared to those required for intramolecular reactions. However, 2-quinolones bearing a directing group at

Department of Basic Medicinal Sciences, Graduate School of Pharmaceutical Sciences, Nagoya University, Furo-cho Chikusa, Nagoya 464-8603, Japan. E-mail: t-yasui@ps.nagoya-u.ac.jp; yamamoto-yoshi@ps.nagoya-u.ac.jp

† Electronic supplementary information (ESI) available: Experimental details, characterization, spectroscopic data, theoretical calculations, and supporting figures and tables. CCDC 2278040–2278045. For ESI and crystallographic data in CIF or other electronic format see DOI: https://doi.org/10.1039/d3sc03987k

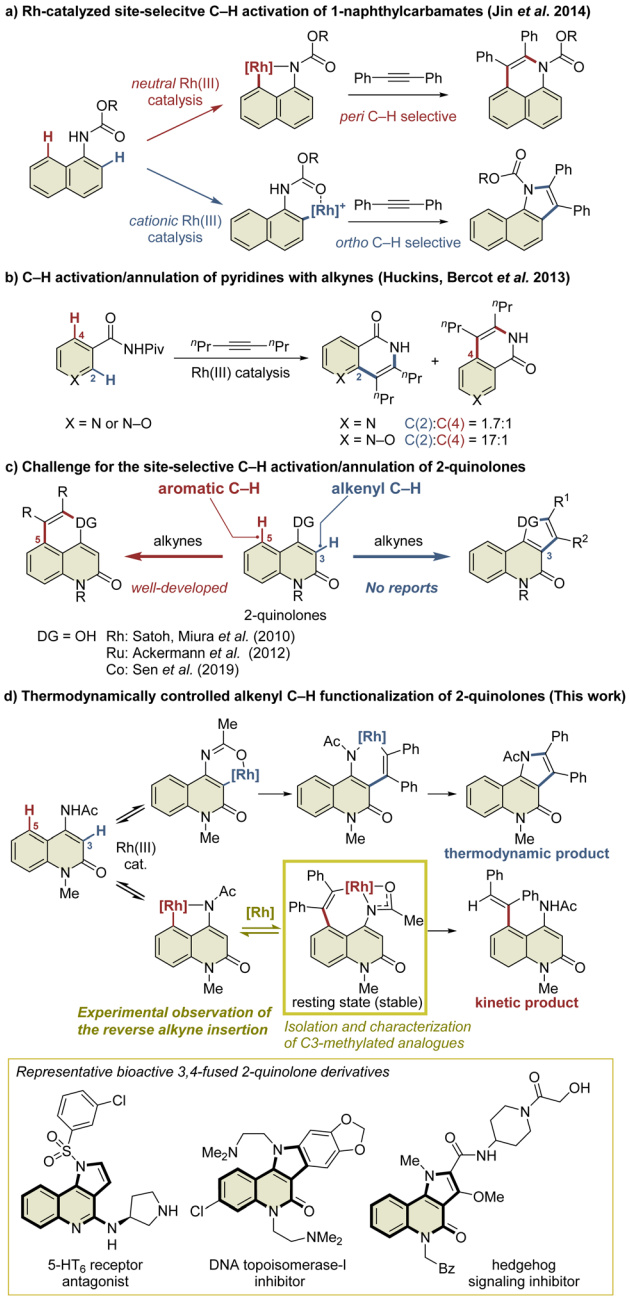

Scheme 1 Site-selective C–H functionalization of aromatic compounds with two cleavable C–H bonds.

the C4-position possess two cleavable C–H bonds: an alkenyl C–H bond at the C3-position and an aromatic C–H bond at the C5-position (Scheme 1c). For selective access to 3,4-fused 2-quinolones, C3-selective C–H functionalization is required. As an effective method of managing this issue, Pd/norbornene-mediated C3-selective C–H functionalizations (the Catellani reaction) of 4-iodo-2-quinolones have recently been developed by the present authors and other research groups.[9,10] However, the related annulation of 4-iodo-2-quinolones with activated alkynes, such as dimethyl acetylenedicarboxylate, can potentially afford both 3,4- and 4,5-fused 2-quinolone products.[11] Thus, the C3-selective annulation of 2-quinolones with alkynes is a formidable challenge, whereas the C5-selective annulation has been well developed.[12]

Herein, we report the Rh(III)-catalyzed highly selective alkenyl C–H functionalization of 4-amino-2-quinolones, providing access to 3,4-fused 2-quinolones (Scheme 1d). The mechanistic study suggested that the present C3-selective annulation reaction proceeds *via* an unprecedented reversible alkyne insertion. In general, the reverse process of alkyne insertion is recognized as an unfavorable process. In fact, only a few examples of β-carbon elimination of alkenylmetal species have been reported to date.[13] Ishii *et al.* reported the β-carbon elimination of Ru or Rh complexes, and indicated that the β-carbon elimination was thermodynamically unfavorable.[13b,c] On the other hand, in the previously reported Rh(III)-catalyzed C–H activation/annulation reactions, the DFT calculations indicated that the β-carbon elimination of alkenylrhodium intermediates required relatively high activation energy, which is estimated to be more than +27 kcal mol^{-1} in most cases.[14] Thus, subsequent processes such as reductive elimination are generally more facile to occur, and the β-carbon elimination of an alkenylrhodium complex is hard to observe, even if possible. Nevertheless, in this study, we have succeeded in the preparation of a key alkenylrhodium intermediate analog and the observation of the β-carbon elimination involving a binuclear Rh complex.

The resulting product has a pyrroloquinolone scaffold, which is found in a number of bioactive compounds such as hedgehog signaling inhibitors,[7b] 5-HT_6 receptor antagonists,[7d] and topoisomerase-I inhibitors.[7e] As an efficient method for the construction of this scaffold, Cai *et al.* have reported the Cu-catalyzed tandem [3 + 2] cycloaddition/C–C coupling of *N*-methyl-*N*-(2-iodophenyl) propiolamides with isocyanides,[15a] although preparation methods of

Table 1 Selected optimization study[a]

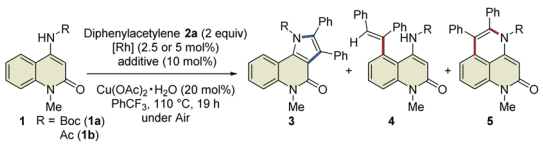

Entry	1	Additive	3 (%)	4 (%)	5 (%)	RSM (%)
1[b]	**1a**	$AgSbF_6$	<10	n.d.	65	0
2[c]	**1a**	—	n.d.	n.d.	78	0
3[c,d]	**1b**	—	63	n.d.	n.d.	0
4	**1b**	—	68	n.d.	n.d.	0
5[e]	**1b**	—	65	5	n.d.	0
6[f]	**1b**	—	n.d.	n.d.	n.d.	92

[a] Reaction conditions: **1** (0.2 mmol), **2a** (0.4 mmol), $[Cp^*RhCl_2]_2$ (2.5 mol%) or $Cp^*Rh(OAc)_2 \cdot H_2O$ (5 mol%), $Cu(OAc)_2 \cdot H_2O$ (20 mol%), $PhCF_3$ (2 mL). For details of the optimization study, see Tables S1 and S2. The isolated yields are reported. n.d. = not detected. [b] Yields were determined by ^1H NMR spectroscopy of the crude mixture. [c] 1,2-Dichloroethane was used as the solvent instead of $PhCF_3$. [d] 2 equiv. of $Cu(OAc)_2 \cdot H_2O$ was used under Ar atmosphere. [e] $Cp^*Rh(OAc)_2 \cdot H_2O$ was used instead of $[Cp^*RhCl_2]_2$. [f] AcOH (1 equiv.) was added.

pyrroloquinolone derivatives are still scarce and are mostly based on linear synthesis.[15] However, the preparation of isocyanides generally requires several steps, most of which still rely on the dehydration of formamides with highly electrophilic dehydration reagents such as $POCl_3$ and *p*-TsCl.[16] In addition, this method is unsuitable for the collective synthesis of diverse products because lengthy synthetic manipulations are required for the introduction of different substituents on the pyrrole ring. Compared with this method, in the present Rh-catalyzed annulation reaction, numerous alkynes can be used as stable and readily available reagents, allowing quick access to diverse pyrroloquinolone derivatives from 4-amino-2-quinolones.

Results and discussion

Reaction development

This study was commenced with the reaction of 4-amino-*N*-Boc-2-quinolone (**1a**) using a cationic Rh(III) catalyst ($[Cp^*RhCl_2]_2$/$AgSbF_6$) to realize C3-selective annulation with diphenylacetylene, based on Jin's report.[4] However, the undesired C5-annulated product **5aa** was selectively obtained in 65% yield,

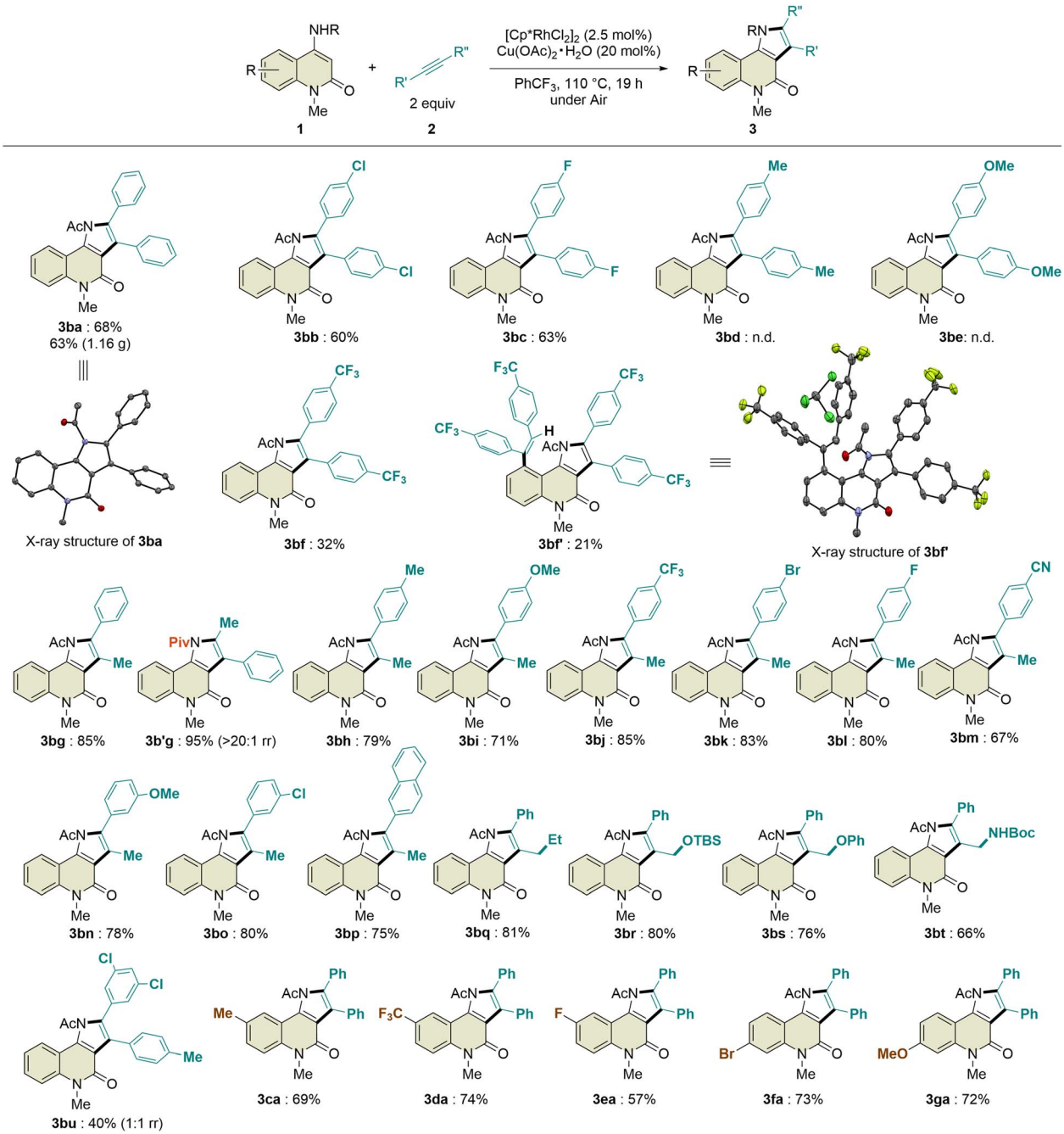

Scheme 2 Substrate scope.

along with several unidentified products (Table 1, entry 1). The use of the neutral Rh(III) catalyst ([Cp*RhCl$_2$]$_2$) also resulted in the selective formation of **5aa** (entry 2). These results indicate that the principle for the site-selective annulation of 1-naphthalenylcarbamates with alkynes is not applicable to the present reaction. Surprisingly, however, the reaction of 4-amino-*N*-acetyl-2-quinolone (**1b**) using the neutral Rh(III) catalyst afforded the desired C3-annulated product **3ba** in 63% yield without the formation of C5-functionalized products (entry 3). An optimization study revealed that the use of benzotrifluoride as the solvent gave the highest yield of **3ba** (entry 4). Notably, when Cp*Rh(OAc)$_2\cdot$H$_2$O was used as the catalyst, **3ba** was obtained in 65% yield, along with C5-functionalized product **4ba** in 5% yield (entry 5); the latter might be generated *via* protodemetalation associated with increasing the amount of acetate derived from the catalyst. However, the reaction did not proceed when one equivalent of acetic acid was added to promote the formation of **4ba** (entry 6).

Substrate scope. The scope of the C3-selective C–H bond activation/annulation reaction was explored under the optimal reaction conditions (Scheme 2). First, various symmetrical internal alkynes were investigated. Diarylacetylenes with halogen substituents, such as di(*p*-chlorophenyl)acetylene (**2b**) and di(*p*-fluorophenyl)acetylene (**2c**), readily reacted with **1b** to afford the desired products **3bb** and **3bc** in 60% and 63% yields, respectively, whereas diarylacetylenes bearing electron-donating groups did not afford the corresponding products (**3bd** and **3be**). Interestingly, the reaction of **1b** with alkyne **2f**, which has two trifluoromethyl groups, produced not only **3bf** but also **3bf′**. The structure of **3bf′** was unambiguously confirmed by X-ray crystallographic analysis. To our delight, the reaction using unsymmetrical internal alkynes **2g–t** proceeded smoothly to afford the corresponding products **3bg–bt** as single regioisomers in 66–85% yields. In contrast, the use of unsymmetrical internal alkyne **2u** possessing 3,5-dichlorophenyl and 4-methylphenyl groups resulted in the yield of **3bu** with a 1 : 1 regioisomeric ratio. In addition, 4-octyne and phenylacetylene were not tolerated in this transformation. Regarding the substituents on the benzene ring of the 2-quinolone scaffold, methyl, trifluoromethyl, fluoro, bromo, and methoxy groups at the C6- or C7-positions were compatible with this reaction, affording the desired products **3ca–ga** in 57–74% yields with excellent site-selectivity. Remarkably, the introduction of a pivaloyl group instead of the acetyl group in **1b** led to the formation of **3b′g** in 95% yield with excellent regioselectivity (>20 : 1 rr), which is probably due to the steric hindrance between the *tert*-butyl and phenyl groups. To evaluate the potential utility of this reaction, we performed a scale-up experiment, which produced 1.16 g of **3ba** without a significant decrease in the yield (63%).

Mechanistic study. To gain insight into the reaction mechanism, several control experiments were performed. First, **1a** was subjected to the standard reaction conditions in the presence of excess methanol-d_4 (Scheme 3). Deuterium incorporation was observed only at the C5-position, indicating that the site-selectivity was determined during the C–H activation step. In sharp contrast, hydrogen/deuterium exchange with **1b** led to deuterium incorporation at both the C3- and C5-positions,

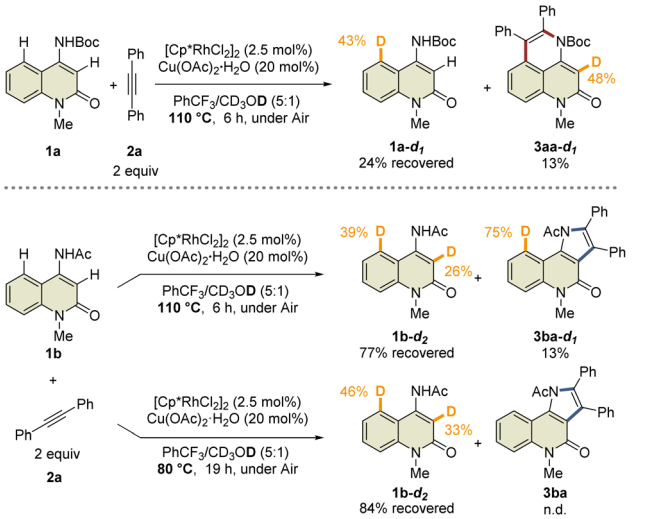

Scheme 3 Analysis of hydrogen/deuterium exchange.

indicating that these C–H bonds could be reversibly cleaved and that C–H activation was not the selectivity-determining step. It was also determined that the C–H activation step was not turnover-limiting because deuterium incorporation was observed even at 80 °C, where the reaction did not proceed.

During the reaction optimization study, we found that not only C3-functionalized product **3ba** but also C5-functionalized product **4ba** were obtained when Cp*Rh(OAc)$_2\cdot$H$_2$O was used as the catalyst (Table 1, entry 5), indicating that alkyne insertion can also occur at the C5-position. Interestingly, lowering the reaction temperature to 100 °C led to an increase in the ratio of **4ba** to **3ba** (Fig. 1a). Furthermore, the same reaction conducted at 70 °C for 6 d afforded **3ba** and **4ba** in 29% and 23% NMR yields, respectively. These results clearly show that **3ba** was

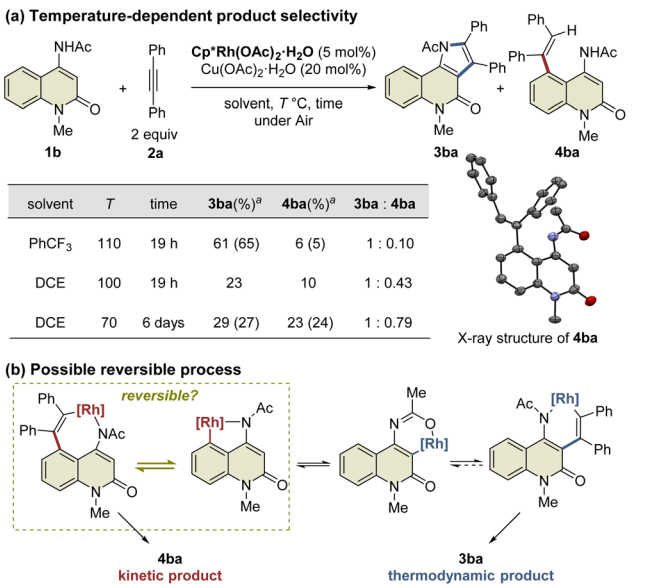

Fig. 1 Temperature-dependence of the reaction. [a]Yields are determined by ^{1}H NMR. Isolated yields are shown in parentheses.

formed under thermodynamic control, whereas **4ba** was formed under kinetic control. Based on these results, we assumed that the alkyne insertion into the five-membered rhodacycle intermediate generated by C5–H activation is a reversible process (Fig. 1b). Although the β-carbon elimination from an alkenylmetal complex is very rare, Ishii *et al.* recently reported that a related seven-membered rhodacycle undergoes an exchange reaction of the alkenyl unit through β-carbon elimination.[13c] Similar alkyne deinsertion could also occur in the present reaction system.

To prove this hypothesis, we performed an NMR experiment using **1b** and **2a-d_{10}** in the presence of a stoichiometric amount of Cp*Rh(OAc)$_2$·H$_2$O as a preliminary investigation. Triethylamine was used as an additive to suppress the protodemetalation. When we monitored the progress of the reaction at 40 °C in $CDCl_3$, two different species, which might be rhodacycle intermediates, other than **3ba-d_{10}** and **4ba-d_{10}**, were observed immediately after initiation of the reaction (Fig. 2a). To our delight, one of these intermediates was isolated by silica gel column chromatography, and X-ray crystallographic analysis

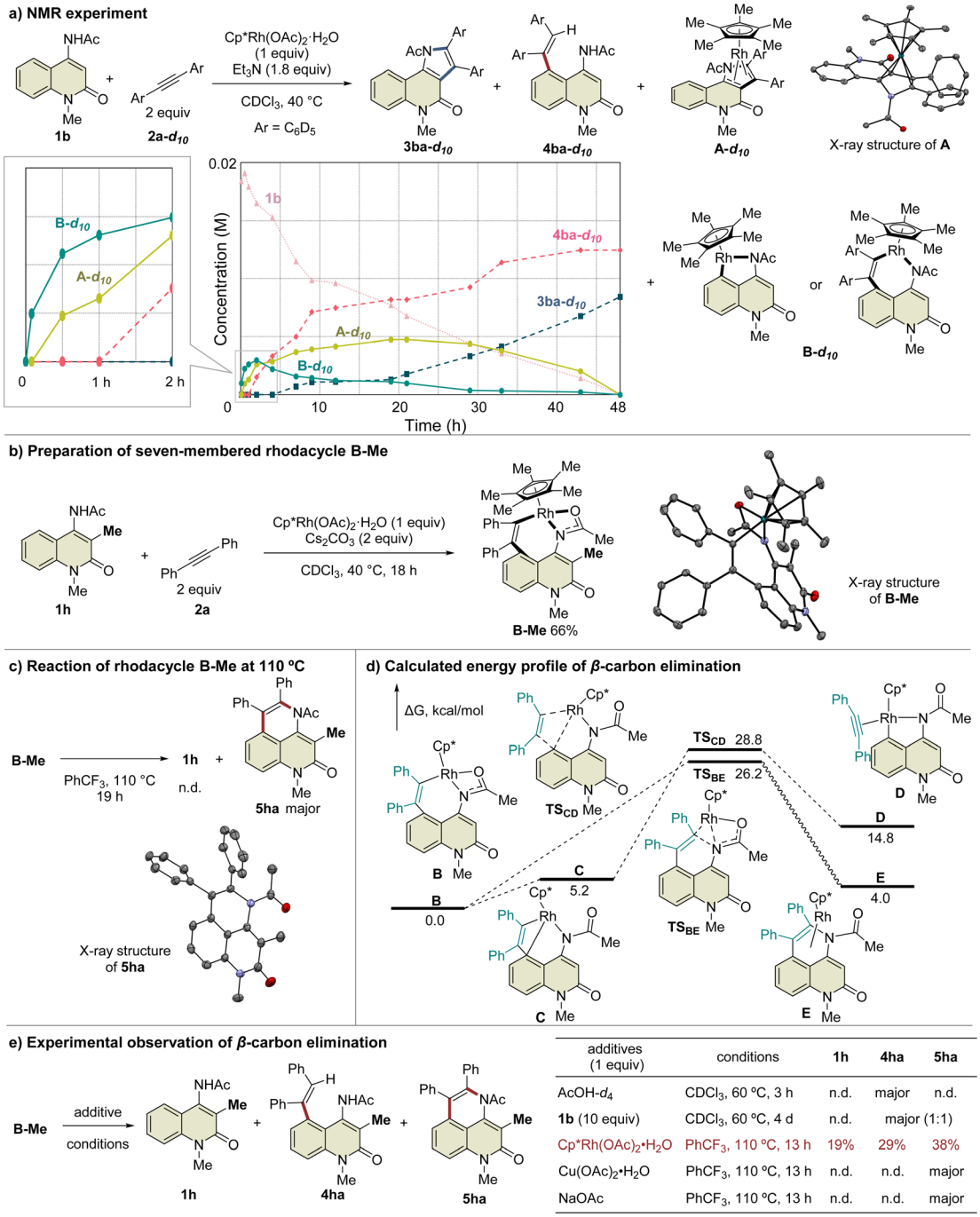

additives (1 equiv)	conditions	1h	4ha	5ha
AcOH-d_4	$CDCl_3$, 60 °C, 3 h	n.d.	major	n.d.
1b (10 equiv)	$CDCl_3$, 60 °C, 4 d	n.d.	major (1:1)	
Cp*Rh(OAc)$_2$•H$_2$O	$PhCF_3$, 110 °C, 13 h	19%	29%	38%
Cu(OAc)$_2$•H$_2$O	$PhCF_3$, 110 °C, 13 h	n.d.	n.d.	major
NaOAc	$PhCF_3$, 110 °C, 13 h	n.d.	n.d.	major

Fig. 2 Mechanistic study involving rhodacycle intermediates.

revealed the structure to be the rhodium sandwich complex **A-d_{10}** with an η^4-pyrrole ligand. However, another intermediate **B-d_{10}** could not be isolated because of its instability. In the NMR experiment, a distinctive ^{1}H NMR signal of the alkenyl proton derived from intermediate **B-d_{10}** was observed at δ 6.35 ppm as a singlet (Fig. S7†). In addition, the corresponding signal of the Cp* methyl groups was also observed at δ 1.32 ppm as a singlet. Based on these observations, we assumed that intermediate **B-d_{10}** might be a five-membered rhodacycle generated by C5–H activation or a seven-membered rhodacycle formed by subsequent alkyne insertion. Reaction monitoring by ^{1}H NMR revealed the formation of a small amount of rhodacycle **B-d_{10}** over a long period of time, suggesting that this intermediate might be in a resting state and gradually evolved into **4ba-d_{10}** *via* protodemetalation or **3ba-d_{10}** through the regeneration of **1b** in equilibrium. To obtain further information regarding intermediate **B**, we designed a C3-methylated 2-quinolone **1h** to prevent the C3-metalation, in order to selectively prepare the corresponding rhodacycle intermediate (Fig. 2b). The treatment of **1h** with Cp*Rh(OAc)$_2$·H$_2$O (1 equiv.) and **2a** (2 equiv.) at 40 °C in $CDCl_3$ led to a rapid and quantitative formation of rhodacycle **B-Me**, for which the ^{1}H NMR signals are similar to those of intermediate **B** observed in the NMR experiment (Fig. S7†). Complex **B-Me** was isolated in 66% yield and X-ray crystallographic analysis unambiguously revealed the structure to be a seven-membered rhodacycle. This rhodium complex adopted a three-legged piano stool geometry, in which the amidate moiety coordinates to the Rh center as a κ^2-N,O bidentate ligand.

With the isolated key intermediate analog **B-Me** in hand, we sought to observe the β-carbon elimination experimentally. First, complex **B-Me** was heated to 110 °C in benzotrifluoride; however, **1h** was not obtained, and reductive elimination proceeded to afford **5ha** as the main product (Fig. 2c). To estimate the activation energy for the β-carbon elimination process, DFT calculations were performed at the SMD (DCE) B3LYP-D3(BJ)/6-311++G(d,p)-SDD//B3LYP-D3(BJ)/6-31G(d)-LanL2DZ level of theory. The calculated activation energy for the β-carbon elimination was 28.8 kcal mol^{-1}, whereas that for reductive elimination was 26.2 kcal mol^{-1}, indicating that it is difficult for β-carbon elimination to proceed before reductive elimination (Fig. 2d). Accordingly, we hypothesized that a mediator is required to promote the β-carbon elimination. Several additives utilized in the present catalytic reaction were examined (Fig. 2e and Table S3†). The addition of AcOH-d_4 resulted in protodemetalation to afford only **4ha**. When an excess amount of **1b** was used, 1 : 1 mixture of **4ha** and **5ha** were observed while **1h** was not detected. Finally, we found that the addition of Cp*Rh(OAc)$_2$·H$_2$O (1 equiv.) promoted β-carbon elimination from **B-Me** to afford **1h** in 19% yield, along with the formation of **4ha** and **5ha**, although the addition of Cu(OAc)$_2$ or NaOAc as an acetate source resulted in the formation of only **5ha**. This suggests that β-carbon elimination from **B-Me** involves a binuclear (or polynuclear) Rh complex, although further investigations are required to elucidate the details of the mechanism of β-carbon elimination in the catalytic reaction process.

A plausible mechanism based on these results is illustrated in Scheme 4. Initially, complex **I′** is formed by the coordination of the Rh catalyst to the amide nitrogen of **1b**, followed by the formation of five-membered rhodacycle **II′** *via* C5–H activation. Subsequent alkyne insertion provides seven-membered rhodacycle **B**, which is a reversible process that involves another Rh catalyst. On the other hand, C3–H activation proceeds *via* the coordination of the Rh catalyst to the amide oxygen to form the six-membered rhodacycle **II**. All these processes are reversible, and complex **B** is in a resting state. A catalytic amount of acetic acid generated *in situ* can protonate complex **B** (or the binuclear Rh complex) to afford **4ba** under kinetic control, while alkyne insertion and reductive elimination from complex **II** proceed to afford the thermodynamic product **3ba**. In the above-mentioned NMR experiment, complex **B** was formed much faster than the **3ba**-Rh(I) complex (complex **A**) in the initial period of the reaction (Fig. 2a), and no NMR signals

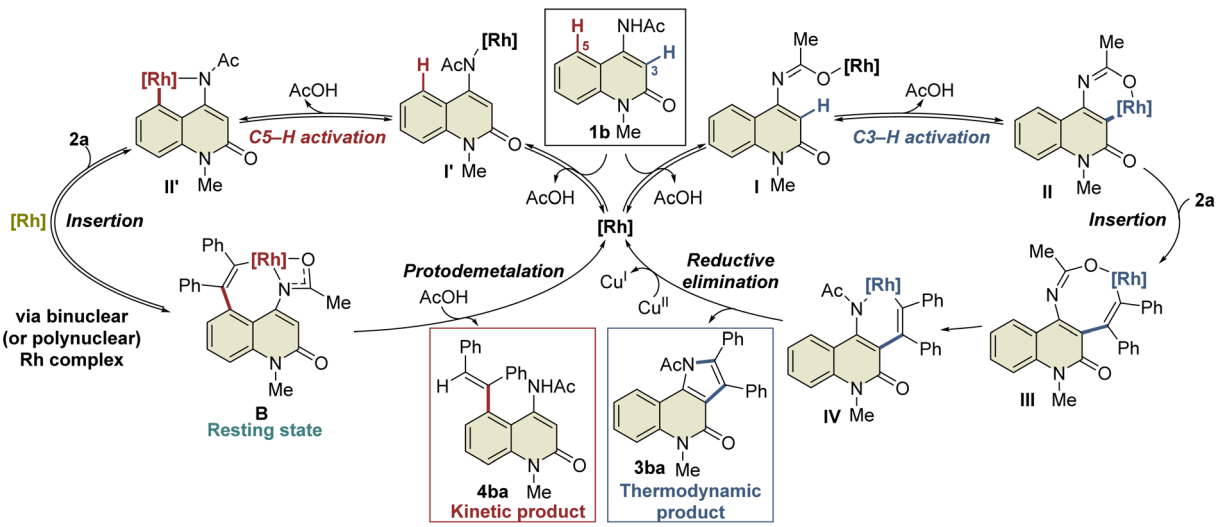

Scheme 4 Proposed reaction mechanism.

corresponding to intermediates **III** or **IV** were detected during the experiment. These results indicate that alkyne insertion from intermediate **II** may be a relatively slow process while reductive elimination from intermediate **IV** may occur more easily. Moreover, because of the low concentration of acetic acid in the catalytic process, protodemetalation from complex **B** is probably much slower than alkyne insertion and reductive elimination from intermediate **II**, allowing the smooth progress of C3-selective functionalization at the elevated temperature.

Conclusions

In summary, we established an efficient method for preparing 3,4-fused 2-quinolones *via* the Rh(III)-catalyzed selective alkenyl C–H functionalization of 4-amino-2-quinolones bearing an *N*-acetyl group as a directing group. This protocol has a wide substrate scope, including unsymmetrical internal alkynes, with complete regioselectivity. Several control experiments using an isolated key intermediate analog suggested that the reaction process involves an unprecedented reversible alkyne insertion process, leading to the simultaneous existence of key intermediates for both C3- and C5-functionalization in equilibrium. Alkyne insertion and reductive elimination from the C3-metalated intermediate may occur more readily than protodemetalation (or reductive elimination) from the seven-membered rhodacycle intermediate leading to C5-functionalization, allowing selective functionalization of the alkenyl C3–H bond over the aromatic C5–H bond. Further studies, including theoretical calculations, to elucidate the details of the reaction process are underway in our laboratory.

Data availability

Data for the crystal structure reported in this paper have been deposited at the Cambridge Crystallographic Data Centre (CCDC) under the deposition number 2278040 (for **3ba**), 2278041 (for **3bf′**), 2278042 (for **4ba**), 2278043 (for **5ha**), 2278044 (for **A**), and 2278045 (for **B-Me**). All other data including experimental procedures, compound characterization, NMR spectra, theoretical calculations, and supporting figures and tables are recorded in the ESI.†

Author contributions

N. H. performed experiments, computational studies, and X-ray crystal structure analysis. N. H. and T. Y. wrote the manuscript. T. Y. and Y. Y designed, advised, and directed the project. All authors edited the manuscript.

Conflicts of interest

There are no conflicts to declare.

Acknowledgements

This research was partially supported by the Platform Project for Supporting Drug Discovery and Life Science Research (Basis for Supporting Innovative Drug Discovery and Life Science Research (BINDS) from AMED under Grant Number JP23ama121044) and JSPS KAKENHI (Grant Number JP21K05051). The computations were carried out on the supercomputer of the Research Center for Computational Science, Okazaki, Japan (Project: 23-IMS-C125). We thank Dr Shuhei Ohmura for carrying out the X-ray crystallographic analysis.

Notes and references

1 For recent reviews, see: (*a*) R. Zhu, M. E. Farmer, Y. Chen and J. Yu, *Angew. Chem., Int. Ed.*, 2016, **55**, 10578–10599; (*b*) T. Brandhofer and O. García Mancheño, *Eur. J. Org Chem.*, 2018, **2018**, 6050–6067; (*c*) A. Baccalini, G. Faita, G. Zanoni and D. Maiti, *Chem. - Eur. J.*, 2020, **26**, 9749–9783; (*d*) O. Baudoin, *Angew. Chem., Int. Ed.*, 2020, **59**, 17798–17809; (*e*) Y. Zhang and M. Szostak, *Chem. - Eur. J.*, 2022, **28**, e202104278.

2 For selected reviews, see: (*a*) R. He, Z.-T. Huang, Q.-Y. Zheng and C. Wang, *Tetrahedron Lett.*, 2014, **55**, 5705–5713; (*b*) X. Cui, J. Mo, L. Wang and Y. Liu, *Synthesis*, 2015, **47**, 439–459; (*c*) P. Gandeepan and C.-H. Cheng, *Chem.–Asian J.*, 2016, **11**, 448–460; (*d*) Y. Yang, K. Li, Y. Cheng, D. Wan, M. Li and J. You, *Chem. Commun.*, 2016, **52**, 2872–2884; (*e*) A. Peneau, C. Guillou and L. Chabaud, *Eur. J. Org Chem.*, 2018, **2018**, 5777–5794; (*f*) C. Wang, F. Chen, P. Qian and J. Cheng, *Org. Biomol. Chem.*, 2021, **19**, 1705–1721; (*g*) A. Saha, M. Shankar, S. Sau and A. K. Sahoo, *Chem. Commun.*, 2022, **58**, 4561–4587.

3 (*a*) Á. M. Martínez, J. Echavarren, I. Alonso, N. Rodríguez, R. G. Arrayás and J. C. Carretero, *Chem. Sci.*, 2015, **6**, 5802–5814; (*b*) K. Elumalai and W. K. Leong, *Tetrahedron Lett.*, 2018, **59**, 113; (*c*) T. P. Pabst, J. V. Obligacion, É. Rochette, I. Pappas and P. J. Chirik, *J. Am. Chem. Soc.*, 2019, **141**, 15378–15389; (*d*) R. A. Alharis, C. L. Mcmullin, D. L. Davies, K. Singh and S. A. Macgregor, *J. Am. Chem. Soc.*, 2019, **141**, 8896–8906; (*e*) D. Prim and B. Large, *Synthesis*, 2020, **52**, 2600–2612.

4 X. Zhang, W. Si, M. Bao, N. Asao, Y. Yamamoto and T. Jin, *Org. Lett.*, 2014, **16**, 4830–4833.

5 (*a*) R. B. Bedford, S. J. Durrant and M. Montgomery, *Angew. Chem., Int. Ed.*, 2015, **54**, 8787–8790; (*b*) J. A. Leitch, Y. Bhonoah and C. G. Frost, *ACS Catal.*, 2017, **7**, 5618–5627; (*c*) D. Kang, K. Ahn and S. Hong, *Asian J. Org. Chem.*, 2018, **7**, 1136–1150; (*d*) A. Biswas, S. Maity, S. Pan and R. Samanta, *Chem.–Asian J.*, 2020, **15**, 2092–2109; (*e*) A. Corio, C. Gravier-Pelletier and P. Busca, *Molecules*, 2021, **26**, 5467; (*f*) Y. Yamamoto in *Handbook of CH-Functionalization*, ed. D. Maiti, Wiley, 2022.

6 (*a*) J. R. Huckins, E. A. Bercot, O. R. Thiel, T.-L. Hwang and M. M. Bio, *J. Am. Chem. Soc.*, 2013, **135**, 14492–14495; (*b*) S. R. Neufeldt, G. Jiménez-Osés, J. R. Huckins, O. R. Thiel and K. N. Houk, *J. Am. Chem. Soc.*, 2015, **137**, 9843–9854.

7 (*a*) C. A. Leach, T. H. Brown, R. J. Ife, D. J. Keeling, S. M. Laing, M. E. Parsons, C. A. Price and K. J. Wiggall, *J. Med. Chem.*, 1992, **35**, 1845–1852; (*b*) T. Ohashi, Y. Oguro,

T. Tanaka, Z. Shiokawa, S. Shibata, Y. Sato, H. Yamakawa, H. Hattori, Y. Yamamoto, S. Kondo, M. Miyamoto, H. Tojo, A. Baba and S. Sasaki, *Bioorg. Med. Chem.*, 2012, **20**, 5496–5506; (*c*) Z. Fu, K. Jiang, T. Zhu, J. Torres and Y. R. Chi, *Angew. Chem., Int. Ed.*, 2014, **53**, 6506–6510; (*d*) K. Grychowska, G. Satała, T. Koz, A. Partyka, E. Colacino, S. Chaumont-Dubel, X. Bantreil, A. Wesołowska, M. Pawłowski, J. Martinez, P. Marin, G. Subra, A. J. Bojarski, F. Lamaty, P. Popik and P. Zajdel, *ACS Chem. Neurosci.*, 2016, **7**, 972–983; (*e*) W.-Y. Hsueh, Y.-S. E. Lee, M.-S. Huang, C.-H. Lai, Y.-S. Gao, J.-C. Lin, Y.-F. Chen, C.-L. Chang, S.-Y. Chou, S.-F. Chen, Y.-Y. Lu, L.-H. Chang, S. F. Lin, Y.-H. Lin, P.-C. Hsu, W.-Y. Wei, Y.-C. Huang, Y.-F. Kao, L.-W. Teng, H.-H. Liu, Y.-C. Chen, T.-T. Yuan, Y.-W. Chan, P.-H. Huang, Y.-T. Chao, S.-Y. Huang, B.-H. Jian, H.-Y. Huang, S.-C. Yang, T.-H. Lo, G.-R. Huang, S.-Y. Wang, H.-S. Lin, S.-H. Chuang and J.-J. Huang, *J. Med. Chem.*, 2021, **64**, 1435–1453.

8 (*a*) L. M. Pardo, A. M. Prendergast, M.-T. Nolan, E. Ó Muimhneacháin and G. P. Mcglacken, *Eur. J. Org Chem.*, 2015, **2015**, 3540–3550; (*b*) K. Mackey, L. M. Pardo, A. M. Prendergast, M.-T. Nolan, L. M. Bateman and G. P. Mcglacken, *Org. Lett.*, 2016, **18**, 2540–2543; (*c*) C. Cheng, W.-W. Chen, B. Xu and M.-H. Xu, *J. Org. Chem.*, 2016, **81**, 11501–11507; (*d*) X. Li, L. Hu, S. Ma, H. Yu, G. Lu and T. Xu, *ACS Catal.*, 2023, **13**, 4873–4881.

9 (*a*) Y. Yamamoto, T. Murayama, J. Jiang, T. Yasui and M. Shibuya, *Chem. Sci.*, 2018, **9**, 1191–1199; (*b*) X.-M. Chen, C. Zhu, D.-F. Chen and L.-Z. Gong, *Angew. Chem., Int. Ed.*, 2021, **60**, 24844–24848.

10 For related examples, see: (*a*) C. Blaszykowski, E. Aktoudianakis, C. Bressy, D. Alberico and M. Lautens, *Org. Lett.*, 2006, **8**, 2043–2045; (*b*) Y. Shang, C. Wu, Q. Gao, C. Liu, L. Li, X. Zhang, H.-G. Cheng, S. Liu and Q. Zhou, *Nat. Commun.*, 2021, **12**, 2988–2998.

11 Y. Yamamoto, J. Jiang and T. Yasui, *Chem. - Eur. J.*, 2020, **26**, 3749–3757.

12 (*a*) S. Mochida, M. Shimizu, K. Hirano, T. Satoh and M. Miura, *Chem.–Asian J.*, 2010, **5**, 847–851; (*b*) V. S. Thirunavukkarasu, M. Donati and L. Ackermann, *Org. Lett.*, 2012, **14**, 3416–3419; (*c*) P. K. Dutta, M. K. Ravva and S. Sen, *J. Org. Chem.*, 2019, **84**, 1176–1184.

13 (*a*) M. Etienne, R. Mathieu and B. Donnadieu, *J. Am. Chem. Soc.*, 1997, **119**, 3218–3228; (*b*) Y. Ikeda, Y. Mutoh, K. Imai, N. Tsuchida, K. Takano and Y. Ishii, *Organometallics*, 2013, **32**, 4353–4358; (*c*) T. Iwamoto, K. Shibuya, T. Takakuwa, T. Kuwabara and Y. Ishii, *Organometallics*, 2022, **41**, 182–186.

14 (*a*) W. Wu, Y. Liu and S. Bi, *Org. Biomol. Chem.*, 2015, **13**, 8251–8260; (*b*) W.-J. Chen and Z. Lin, *Organometallics*, 2015, **34**, 309–318; (*c*) R. Thenarukandiyil, S. K. Gupta and J. Choudhury, *ACS Catal.*, 2016, **6**, 5132–5137; (*d*) M. Zhang and G. Huang, *Chem. - Eur. J.*, 2016, **22**, 9356–9365; (*e*) Y.-F. Yang, K. N. Houk and Y.-D. Wu, *J. Am. Chem. Soc.*, 2016, **138**, 6861–6868; (*f*) L. Han, X. Zhang, X. Wang, F. Zhao, S. Liu and T. Liu, *Org. Biomol. Chem.*, 2017, **15**, 3938–3946.

15 (*a*) F. Zhou, J. Liu, K. D. Jinsong and Q. Cai, *J. Org. Chem.*, 2011, **76**, 5346–5353; (*b*) T. C. T. Ho and K. Jones, *Tetrahedron*, 1997, **53**, 8278–8294; (*c*) G. T. Manh, H. Bakkali, L. Maingot, M. Pipelier, U. Joshi, J. P. Pradére, S. Sabelle, R. Tuloup and D. Dubreuil, *Tetrahedron Lett.*, 2004, **45**, 5913–5916; (*d*) X. Zhang, L. Huang, H. Peng, F. Ji, X. Li and B. Yin, *Tetrahedron*, 2014, **70**, 5242–5248.

16 K. A. Waibel, R. Nickisch, N. Möhl, R. Selim and M. A. R. Meier, *Green Chem.*, 2020, **22**, 933–941, and the references therein.